Gamma-Ray Emission from Radioactive Isobars

Author

03/16/14

Abstract

Using a high-purity germanium (HPGe) detector, we have successfully measured the gamma-ray emission spectrum for five different radioactive nuclei. The nuclei measured were ^{60}Co, ^{57}Co, ^{137}Cs, ^{54}Mn, and ^{22}Na. Each spectrum was found to be correct, verified using a chart of nuclides. ^{60}Co emits gamma-rays through β^- decay with an energy peak at E_γ = 1332.3 keV with a percent error of .015%. ^{57}Co emits gamma-rays through electron capture with energy peaks at E_γ = 122.1 keV (percent error = 0%), E_γ = 136.5 keV (percent error = 0%), and E_γ = 14.5 keV (percent error = .7%). ^{137}Cs emits gamma-rays through β^- decay with an energy peak at E_γ = 661.5 keV (percent error = 0.03%). ^{54}Mn decays through electron capture with an energy peak of E_γ = 834.2 keV (percent error = .07%). ^{22}Na decays through β^+ decay (pair production) with an energy of E_γ = 1274.5 keV (percent error = 0%). In addition to verifying the gamma-ray spectrum for each radioactive species, we were also able to determine the manner by which each nuclide decayed into its respective daughter nuclei.

Introduction

Our goals for this lab were to measure the gamma-ray emmission spectrum for various radioactive nuclei and to determine the decay process of each nuclei. The techniques of gamma-ray spectroscopy have been instrumental in obtaining fundamental information concerning nuclear structure, cosmic rays, elementary particles and the physics of solids. They have played an increasingly important role in medical and biological research thanks to radioactive tracers.

Beta Decay

Gamma-ray emission from radioactive nuclei can occur in many ways. One such method of gamma-ray emission is through beta decay. The nucleus of an atom is composed primarily of protons and neutrons. For radioactive nuclei, neutrons may decay into a proton (p) and emit both β^- particles (electrons, e^-) and anti-neutrinos (ν).

$$n \rightarrow p + e^- + \bar{\nu}_e$$

When this occurs, the nuclear charge changes by one electronic charge. The parent nuclei (Z, A) transitions to a daughter nuclei (Z+1, A), where Z is the number of protons in the nucleus (atomic number) and A is the sum of protons and neutrons (mass number). The daughter nuclei may be left in an excited stated (Z+1, A)*, which will then decay to the ground state with the emission of a gamma-ray.

Positron Decay

Another decay process is positron decay. In this process, (Z, A) transitions to (Z-1, A) with the emission of a positron (e^+). The positron is the antiparticle of the electron. It has the same mass but with a positive charge instead of a negative charge. The decay equation is

$$p \rightarrow n + e^+ + \nu_e$$

where ν_e is the neutrino. Because the positron is anti-matter, it quickly loses kinetic energy and stops near an electron due to the Coulomb attraction of opposite charges. Therefore, an annihilation takes place

$$e^- + e^+ \rightarrow energy$$

where the energy is emitted in the form of two γ rays in order to conserve momentum. The sum of the two gamma-ray energies must equal the energy when the positron and electron annihilate. The usual case when two gamma-rays are emitted is

$$E_\gamma = M_e c^2 = 0.511\ MeV.$$

Electron Capture

In the third decay scheme, we observe another instance where the atomic number decreases by one charge, i.e. (Z, A) transitions to (Z-1, A). Electron capture occurs when the nucleus captures one of the electrons in the outer K shell. The K shell electrons of high Z nuclei are relatively close enough to the nucleus that they spend part of their existence in the nucleus. The reaction equation is

$$p + e^- \rightarrow n + \nu_e$$

The hole left behind from the captured K-electron is filled by another electron from a higher shell with the emission of a monoenergetic x-ray. The daughter nuclei may still be in an excited state and will decay with the emission of a monoenergetic gamma-ray.

The daughter nuclei of each decay scheme each have the same mass number (A) as their respective parent nuclei. The parent and daughter nuclei are isobars.

Experimental Design and Procedure

In our experiment, we needed a detector with an output that is proportional to the energy of the incident particle. This ensured that we observed different energy values of gamma-rays emitted from the nuclei we measured.

Ge(Li) and HPGe Detectors

Lithium-drifted germanium (Ge(Li)) detectors provided us with the resolution required to measure the gamma-ray emission spectra. Ge(Li) detectors are an improvement over the previously used thalium-doped sodium iodide detectors (NaI(Tl)). Figure 1 shows a graph of the three most important gamma interactions for both Ge and Si detectors. For this experiment we considered only the Ge detector curves.

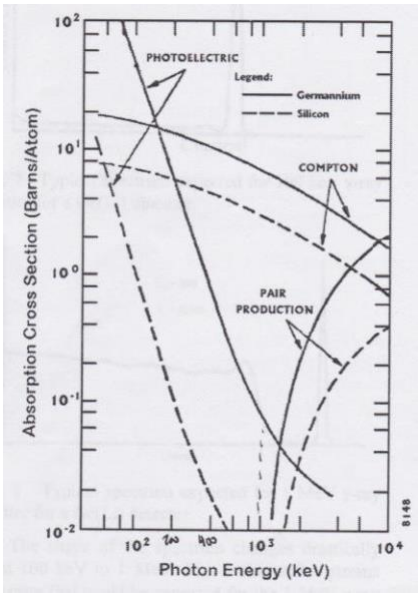

Figure 1: Relative probability of each of the three types of interactions as a function of energy

To determine spectra from calibrating pulse distributions, it is sufficient to understand the main features in the spectra of monoenergetic gamma-rays: full-energy peaks, Compton effects, and annihilation escape peaks (pair production). The full-energy peak is produced by events in which the total energy of the incident photon is absorbed in the detector. Therefore, its position contributes to the energy measurement of the radiation and, through this, often to the identification of the emitting nuclei. For low energy gamma-rays and small detectors, it corresponds to the total energy transfer to a single electron in a photoelectric process; therefore, it is oftened called “photopeak”.

However, according to Figure 1, at medium and high energies and in large detectors, many signals in the fullenergy peak are produced by single or multiple Compton scatterings, followed by the photoelectric absorption of the scattered photon or by pair production when both of the annihilation gammas are absorbed in the detector.

Escape peaks (pair production) occur only if the gamma energy exceeds 1.2 MeV. Annihilation peaks are found only if the gamma transition is preceded by a β^+ decay or $E_\gamma \geq 1.2$ MeV. X-ray escape peaks in scintillation detectors can be resolved from the full-energy peaks only for low energy photons, and the X-rays following the photoelectric absorptions can leave the detector without being absorbed if the interactions took place near the surface, i.e. for low-energy gamma-rays.

Our experiment utilized high-purity germanium (HPGe) detectors. The advantage of the HPGe detector is that it may be stored at room temperature but must be cooled by liquid nitrogen before applying high voltage. An aluminum cylinder contained both the Ge detector and a preamplifier which produced output pulses proportional to the energy from the incident gamma-rays.

Signal Processing

Pulses from the HPGe and preamplifier are further amplified by an Ortec spectroscopy amplifier, model 570. A Canberra Multiport II multichannel analyzer (MCA) pulse height analyzer (PHA) processes these pulses from the spectroscopy

amplifier. The MCA sorts the input pulses into 8,192 equal channels ranging from 0-8 Volts. Figure 2 is a diagram of our experimental set-up.

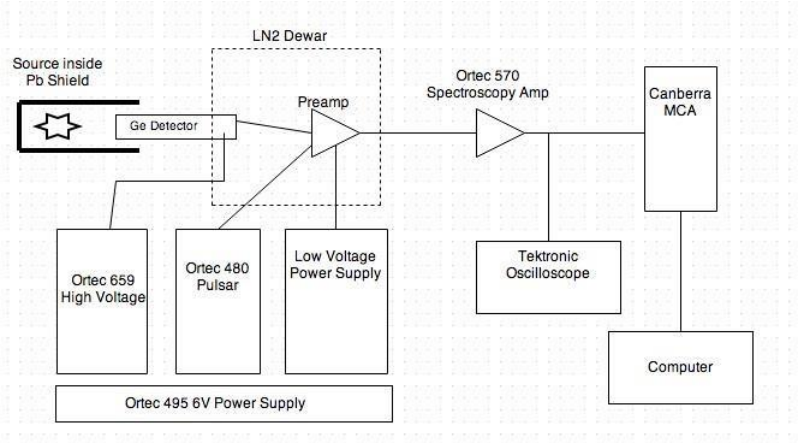

Figure 2: Experimental design for measuring the gamma-ray emission spectrum

After all the instruments were connected, we began the calibration for the channel number by measuring a ^{60}Co source. Using the Genni 2000 Spectroscopy software we calibrated the energy bins by using the 1.17 and 1.33 MeV gamma-ray peaks as reference. Figure 3 shows our resulting calibration curve. Figure 4 and 5 respectively shows the linear and logarithmic spectrum of ^{60}Co.

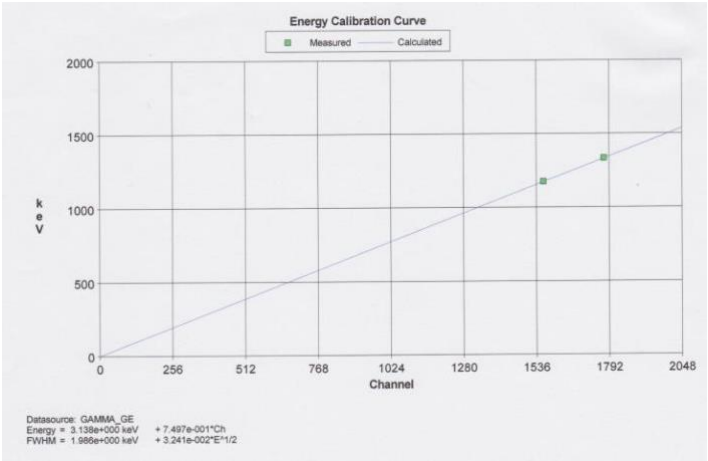

Figure 3: Calibration curve for our experiment

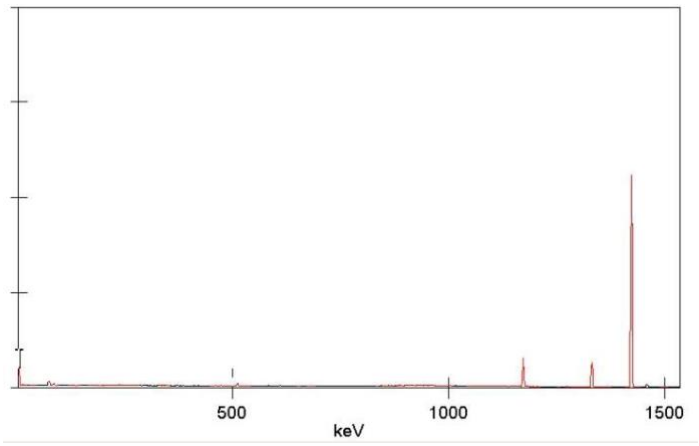

Figure 4: Linear graph of ^{60}Co gamma-ray emission spectrum. The y-axis is gamma-ray counts.

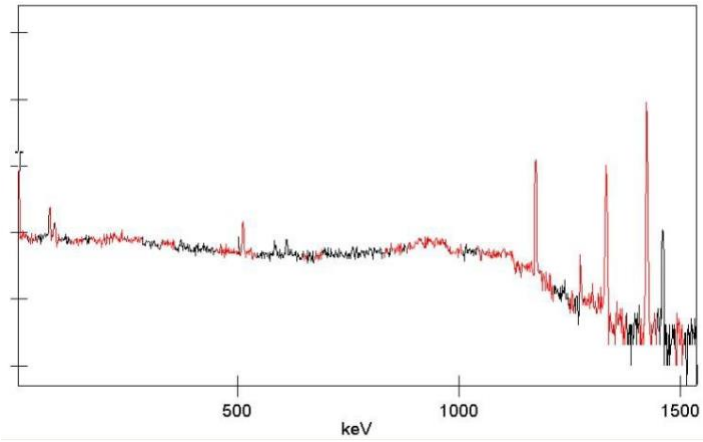

Figure 5: Logarithmic graph of ^{60}Co gamma-ray emission spectrum

From the linear graph we observed the pulser peak at 1424.2 keV with a full-width-half-maximum (FWHM) value of 2.396 keV and an area of 29915 counts ± 0.58%.

To left of the pulser peak, a γ-ray peak was observed at 1332.3 keV with a percent error of 0.015% from the true value of 1332.5 keV. The FWHM value is 2.903 keV and the area of this peak is 4271 counts ± 1.58%.

The last peak is at 1173.2 keV with a FWHM value of 2.927 keV and an area of 4829 counts ± 1.63%.

A Compton edge is observed at an energy of roughly 1000 keV on the logarithmic scaled graph in Figure 5.

Resolution

To obtain the limit on energy resolution due to the electronics R_{elect}, we used the FWHM of the pulser peak. The FWHM for a typical photopeak measured the limit on the energy resolution from both the detector and electronics,

$R_{det+elect}$. Then we used the relation:

$$(R_{det+elect})_2 = (R_{det})_2 + (R_{elect})_2$$

to solve for the resolution from only the detector. Using the gamma-ray peak at 1332.3 keV, the resolution of the detector is 1.639 keV. Using the gamma-ray peak at 1173.2 keV, the resolution of the detector is 1.690 keV. Both values of the detector resolution agree with a difference of 0.03 keV.

Results and Analysis

^{57}Co

Gamma-ray peaks for ^{57}Co were observed at energies of 122.1 keV with a percent error of 0.0%, 136.5 keV with a percent error of 0.0%, and 14.4 keV with a percent error of 0.7%. Due to the output reading of the Genni 2000 software, some measurements were extremely close to the accepted values. Therefore, some of our gamma-ray values yielded a 0.0% error. Figure 6 and 7 show the linear and logarithmic spectrums respectively. Referring to Figure 1, we did not expect to observe a Compton edge due to the low energies of the gamma-rays emitted by ^{57}Co.

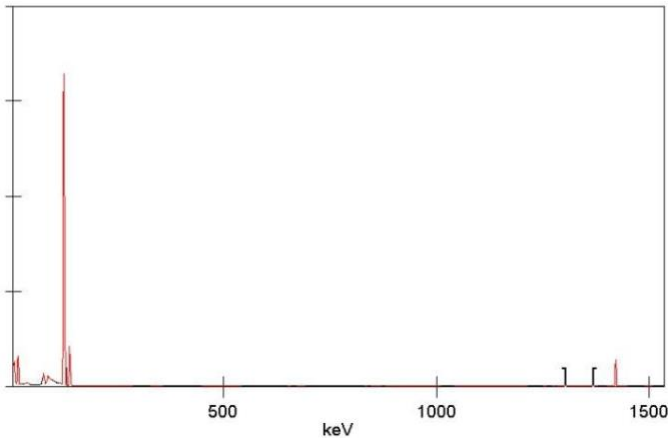

Figure 6: Linear gamma-ray spectrum of ^{57}Co with peak energies at 14.4 keV, 122.1 keV, and 136.5 keV

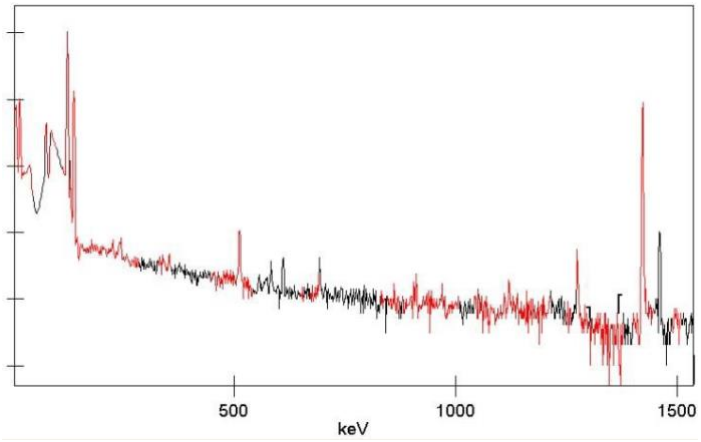

Figure 7: Logarithmic gamma-ray spectrum of ^{57}Co. No Compton edge is observed.

From our measured spectrum of ^{57}Co, we determined that ^{57}Co decays by electron capture.

$$^{57}\text{Co} \rightarrow {}^{57}\text{Fe}$$

Figure 8 shows the decay scheme of ^{57}Co.

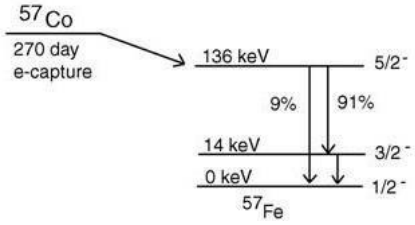

Figure 8: Gamma-ray decay scheme of ^{57}Co

^{137}Cs

A gamma ray peak for ^{137}Cs was observed at 661.5 keV with a percent error of 0.03% from the theoretical value of 661.7 keV. The FWHM value was 2.708 keV. Figures 9 and 10 respectively show the linear and logarithmic gamma-ray emission spectra. The logarithmic reveals a Compton edge at ~500 keV.

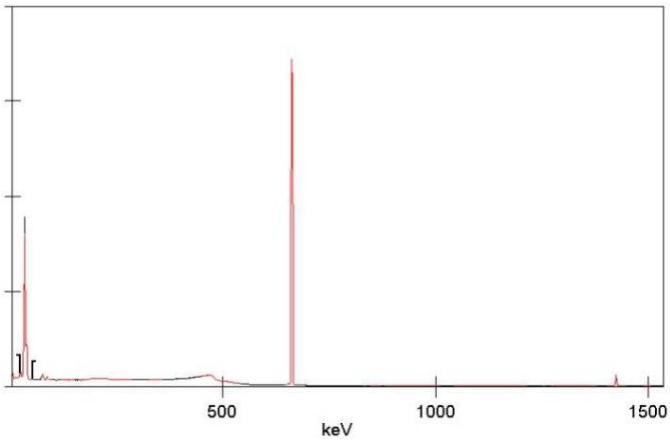

Figure 9: Linear gamma-ray spectrum of ^{137}Cs with a peak energy at 661.5 keV

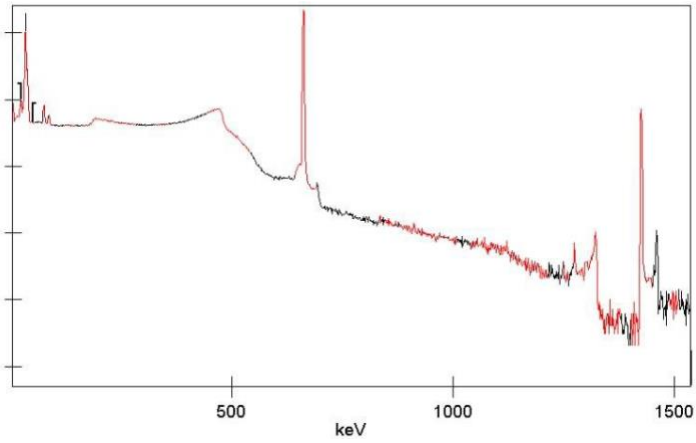

Figure 10: Logarithmic gamma-ray spectrum of 137 with a Compton edge ~500 keV

From our measured spectrum and after consulting a table of nuclides,we determined that ^{137}Cs decays by the process of β^- decay.

$$^{137}\text{Cs} \rightarrow {}^{137}\text{Ba}$$

Figure 11 shows the decay scheme of ^{137}Cs.

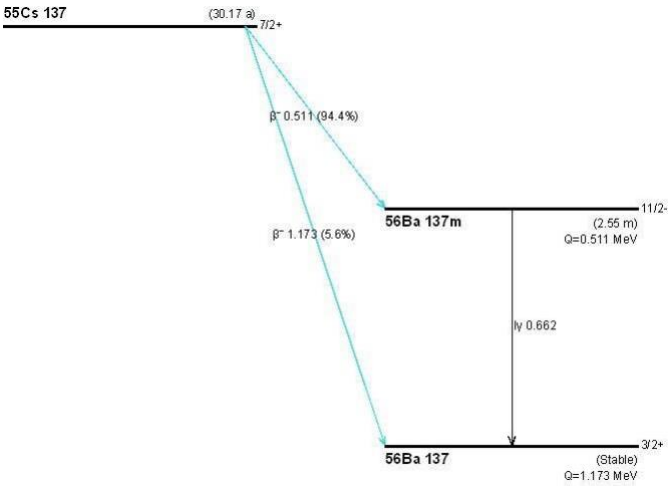

Figure 11: Decay scheme of ^{137}Cs with relative probabilities of the associated pathways for decay

^{54}Mn

A gamma-ray peak for ^{54}Mn was observed at 834.2 keV with a percent error of 0.07%. The FWHM value was 2.850 keV and the peak area was 56816 counts ± 0.46%. A Compton edge was observed at 635.2 keV. Figures 12 and 13 show the linear and logarithmic spectrum for ^{54}Mn respectively.

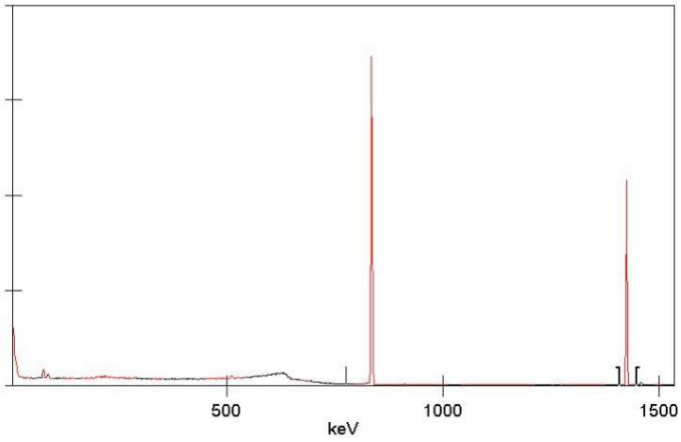

Figure 12: Linear gamma-ray spectrum of ^{54}Mn with a gamma-ray energy of 834.2 keV

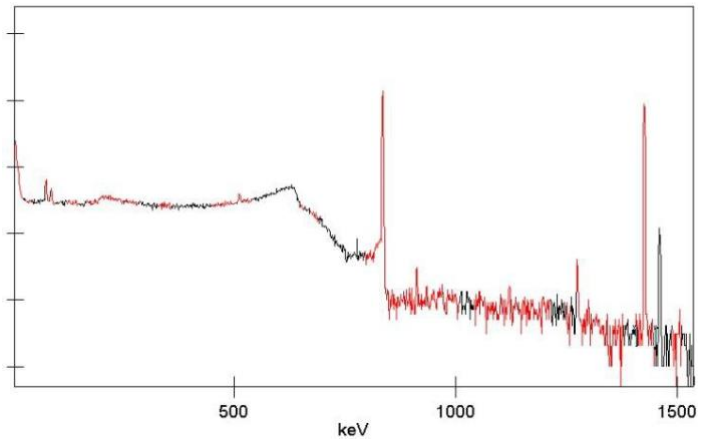

Figure 13: Logarithmic gamma ray spectrum of ^{54}Mn. A Compton edge is revealed at 635.7 keV.

From our measured spectrum and table of nuclides, we determined that ^{54}Mn decays through electron capture.

$$^{54}\text{Mn} \rightarrow {}^{54}\text{Cr}$$

Figure 14 shows the decay scheme of ^{54}Mn.

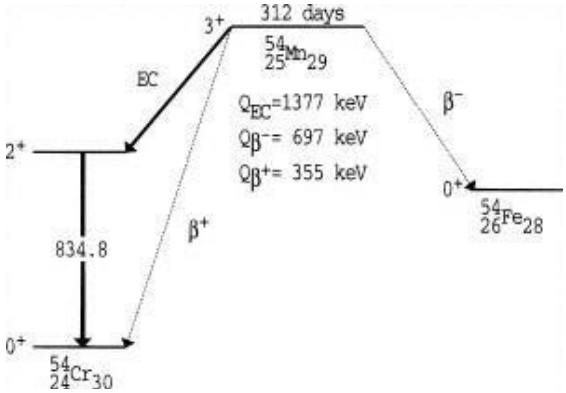

Figure 14: Decay scheme of ^{54}Mn

^{22}Na

A gamma ray peak for ^{22}Na was observed at 1274.5 keV with a percent error of 0.0%. The FWHM value was 2.808 keV and the area of the peak was 32412 counts ± 0.59%. An annihilation peak was also observed at 510.9 keV. The FHWM for the annihilation peak was 3.420 keV with an area of 159437 counts ± 0.28%. Since two gamma-rays are created annihilation occurs, we expected the annihilation peaks to surpass the incident gamma-ray peaks in area. Two Compton edges were observed. The incident gamma-ray Compton edge was observed at 1051.9 keV. The annihilation Compton edge was observed at 338.3 keV. Figures 15 and 16 respectively show the linear and logarithmic spectra of ^{22}Na.

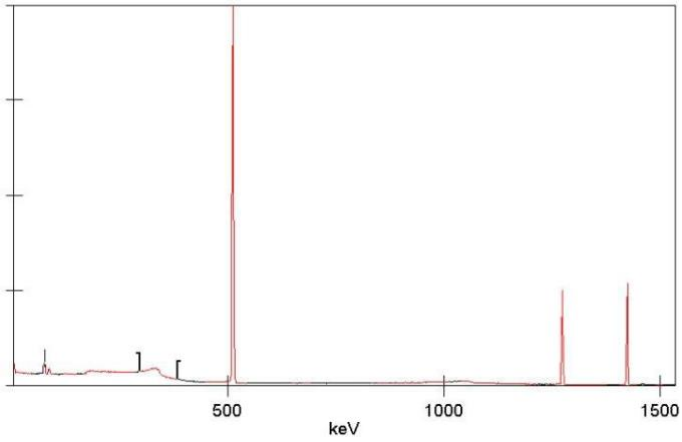

Figure 15: Linear gamma-ray spectrum of ^{22}Na with a gamma-ray peak at 1274.5 keV and annihilation peak at 510.9 keV

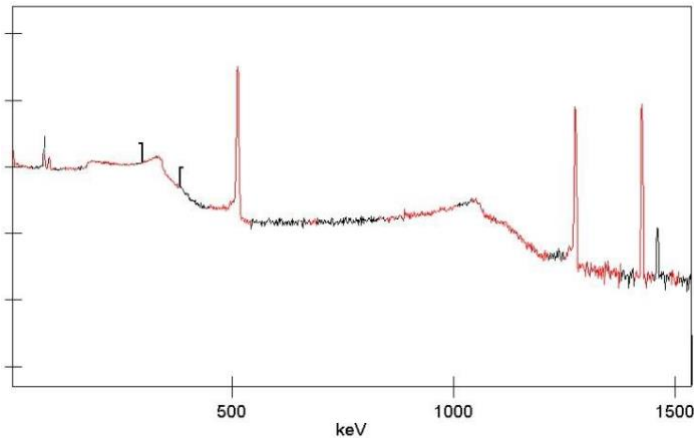

Figure 16: Logarithmic gamma-ray spectrum of ^{22}Na with Compton edges at 338.3 keV and 1051.9 keV

After consulting a table of nuclides and comparing to our measured spectra we determined that ^{22}Na decays through positron decay.

$$^{22}\text{Na} \rightarrow {}^{22}\text{Ne}$$

Figure 17 shows the gamma-ray decay scheme of ^{22}Na.

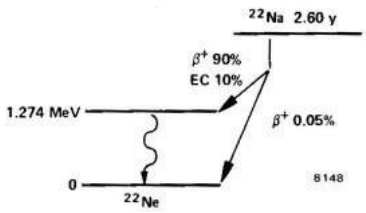

Figure 17: Gamma-ray decay scheme of ^{22}Na

Conclusion

We were successful in our measurement of the gamma-ray emission spectra for ^{60}Co, ^{57}Co, ^{137}Cs, ^{54}Mn, and ^{22}Na. Logarithmic versions of the spectra revealed that Compton edges are prevalent in gamma-ray spectra with relatively higher energies when compared to lower spectra energies. We were also able to determine the process that each radioactive nucleus uses to decay to their respective daughter nuclei. For future studies, it would be advisable to use a program that outputs energy readings with more significant figures. This would ensure a more accurate reading of gamma-ray energies and it would also help prevent percent errors of 0.0%.

Works Cited

1. P. Quittner, *Gamma-Ray Spectroscopy* (John Wiley, New York, 1972)
2. S. M. Shafroth, *Scintillation Spectroscopy of Gamma Radiation* (Gordon and Breach, New York, 1967)
3. *Panel on the Use of Lithium-Drifted Germanium Gammay-Ray Detectors for Research in Nuclear Physics* (International Atomic Energy, 1966)